A flexible tripod fluorescent probe for multiple cations detection and its application in living cells

Wan-Li Xu[a], Jun-Feng Yang[a], Mao-Qian Ran[a], Xi Zeng[a,*], Carl Redshaw[b*], Zhu Tao[a]

[a] Key Laboratory of Macrocyclic and Supramolecular Chemistry of Guizhou Province, School of Chemistry and Chemical Engineering, Guizhou University, Guiyang 550025, China. E-mail: zengxi1962@163.com
[b] Department of Chemistry and Biochemistry, University of Hull, Hull HU6 7RX, UK

Abstract: To the flexible tripod platform tren (tris(2-aminoethyl)amine), a Rhodamine and two naphthalene fluorophores were introduced. The resulting fluorescence probe named **TRN** was fully characterized and employed in cell imaging. Probe **TRN** exhibited high selectivity and excellent sensitivity for the simultaneous fluorescence detection of Zn^{2+}/ Hg^{2+}/ Al^{3+}/ Cu^{2+}. The significant changes in the fluorescence color make naked-eye detection possible. Furthermore, fluorescence imaging experiments of Zn^{2+}/ Hg^{2+}/ Al^{3+}/ Cu^{2+} in living PC3 cells demonstrated its value for practical applications in biological systems.

Key words: flexible tripod probe, Zn^{2+}/ Hg^{2+}/ Al^{3+}/ Cu^{2+} ions detection, cells imaging

1. Introduction

The selective detection of four or more analytes with a single chemosensor is extremely rare owing to the inherent challenge in eliciting unique responses by the molecule in the presence of the different analytes. Such a molecule would involve either having multiple binding sites that give rise to different binding modes, or multiple signal transducing units (e.g., chromophores/ fluorophores/ redox active moieties), multiple read-out modes or any combination of the above. Such a chemsensor would be highly coveted, both in terms of convenience of use and economic value.

A chemosensor would be highly valued for the sensitive detection of metal ion species that play key roles in biological processes, as well as in detecting human toxins and contaminants, especially as there are

increasing demands for sensors in these fields. Among these, the metal ions of mercury, zinc, aluminium and copper are synonymous with various prominent neurological conditions and biological processes. For instance, mercury is a well-known human toxin, capable of serious harm to the skin, nervous and renal systems even at very low levels [1-4]. Zinc is the second most abundant transition-metal ion and plays important roles in a variety of physiological and pathological processes [5-7], and disorder associated with zinc metabolism in biological systems may lead to a variety of diseases such as Alzheimer's disease, diabetes, epilepsy [8-11]. Moreover, Al^{3+} has been associated with conditions such as neuro dementia, Parkinson's disease, Alzheimer's disease and dialysis encephalopathy. Copper ions, as the third most abundant essential trace element after iron and zinc in the human body, also play an important role in various physiological and enzymatic processes [12-14], such as in transforming melanin in skin pigments, assisting cross-linking in collagen, as well as tissue maintenance and repair [15-17]. Excessive copper is also toxic and a major cause for oxidative stress and disorders associated with neurodegenerative diseases including Alzheimer's, Parkinson's, Menkes, Wilson's and prion diseases [18-20]. Thus, there is an urgent need to develop sensors capable of detecting low concentrations of Hg^{2+}, Al^{3+}, Zn^{2+} and Cu^{2+} ions in biological samples.

Fluorescent probes are ideal candidates for both the detection and monitoring of metal ions in a wide variety of samples. This is due to their high sensitivity, fast response, and ability to provide *in situ* and real-time information with high spatial-temporal resolution, and non-destructive detection. During the past two decades, many fluorescent probes have been developed for a variety of biologically and environmentally related targets. However, most of the fluorescent probes that have been reported are of two- or three-ion sensor types that detect for example Fe^{3+}/ Cu^{2+} [21], Ba^{2+}/ Hg^{2+} [22], Zn^{2+}/ Cd^{2+} [23], Cu^{2+}/ Hg^{2+} [24, 25], Pb^{2+}/ Hg^{2+} [26], Zn^{2+}/ Hg^{2+}/ Cu^{2+} [27], Cu^{2+}/ Cysteine [28], Zn^{2+}/ Cd^{2+}/ Hg^{2+} [29], Cr^{3+}/ Al^{3+}/ Fe^{3+} [30, 31]. However, it remains a great challenge for probes to detect even more cations at the same time.

Herein, we report the development of a probe called **TRN**, which possesses unique optical responses towards Zn^{2+}, Al^{3+}, Hg^{2+} and Cu^{2+} ions. It is composed of two *O*-hydroxynaphthalene formaldehyde units and one Rhodamine B moiety bound by a flexible tren linkage, and contains a well-known fluorophore pair allowing for a Förster resonance energy transfer (FRET) process [32-35]. The flexible linkage and the short distance between the fluorophores provide efficient FRET between the fluorophore pair owing to the favorable optical overlap between these two chromophores [36, 37]. The flexible tren linkage not only facilitates the

energy transfer process but also provides versatile binding affinity for the Zn^{2+}, Al^{3+}, Hg^{2+} and Cu^{2+} ions, respectively. The well-separated emission spectra of the donor and acceptor are helpful when distinguishing different analytes. On other hand, the larger pseudo-Stoke's shift of the FRET probe between the maximum emission wavelengths of the naphthalene and Rhodamine moieties favors ruling out the influence of excitation backscattering on the fluorescence detection. Furthermore, the Rhodamine can exhibit outstanding spectroscopic properties and the ring-opening of the spirolactam gives rise to strong fluorescence emission upon combining with the cations [38-40]. The *ortho*-hydroxyl substituted naphthalene Schiff base also gives an off-on optical signal attributed to the C=N isomerization and chelation enhanced fluorescence (CHEF) mechanism [41, 42]. Three different emission processes are likely to occur, these being: (i) donor emission with donor excitation; (ii) acceptor emission with donor excitation; and (iii) acceptor emission with acceptor excitation. These factors highlight probe **TRN**'s potential as a multicolored, multimodal chemosensor.

2. Experimental

2.1 Materials

Deionized water was used throughout the experiments. Other chemicals were purchased from Alfa Aesar Co., Tianjin, China and were used without further purification. The solutions of metal ions were prepared from their perchlorate salts, which were analytical grade.

2.2 Apparatus

Fluorescence spectral measurements were performed on a Cary Eclipse fluorescence spectrophotometer (Agilent Technologies) equipped with a xenon discharge lamp using a 1 cm quartz cell. ^{1}H and ^{13}C NMR spectra were measured on a WNMR-I 500 MHz NMR (Wuhan Institute of Physics and Mathematics, Chinese Academy of Sciences) spectrometer or Bruker AVANCE III 400 NMR spectrometer at room temperature using TMS as an internal standard. MALDI-TOF mass spectra were measured on a Bruker autoflex 3 system. Cell fluorescence imaging was performed using an Olympus IX73 fluorescent inverted microscope.

2.3 Spectral measurements

To a 10 mL volumetric flask containing different amounts of ions, the appropriate amounts of the solution of probe **TRN** were added using a micropipette. For Zn^{2+}, Hg^{2+}, Al^{3+} and Cu^{2+}, the system was then diluted with a CH_3CN/H_2O (95/5) mixed solvent to 10 mL; and then the fluorescence sensing of the ions was conducted. The fluorescence spectra were measured after addition of the ions at room temperature and when equilibrium was reached. Fluorescence measurements were carried out with an excitation and emission slit width of 10 nm.

2.4 Cell culture and fluorescence imaging

PC3 cells are adherent growth cells, and are routinely cultured at 37 °C and 5 % CO_2 saturated humidity in 1640 containing 10 % bovine embryo serum, 100 U/ mL penicillin and 100 μg/ mL streptomycin. The medium was changed every 1 to 2 days, and the cells in the logarithmic growth phase were used for experiments. One day prior to imaging, the cells were seeded in 12-well flat-bottomed plates. The next day, the cells were incubated with 10 μM of probe **TRN** for 45 min at 37 °C. Before incubating with 100 μM Zn^{2+}, Hg^{2+} or Al^{3+} for another 60 min, the cells were rinsed with fresh culture medium three times to remove the remaining sensor, then the fluorescence imaging of intracellular Zn^{2+}, Hg^{2+} and Al^{3+} was observed under an inverted fluorescence microscope. Finally, the cells containing **TRN** were further treated with Cu^{2+} (500 μM) for another 50 min, then the fluorescence imaging was observed under an inverted fluorescence microscope.

2.5 Synthesis of probe **TRN**

The synthetic route to probe **TRN** via the intermediate **TR** was carried out as outlined in Scheme 1:

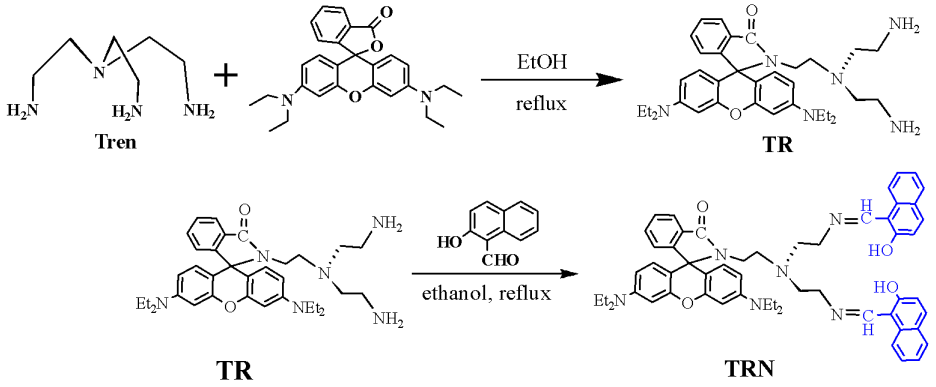

Scheme 1. Synthetic route to the probe **TRN**

Tris(2-aminoethyl)amine (tren) (4.0 g, 27.36 mmol) was dissolved in 20 mL of ethanol. Rhodamine B (1.64 g, 3.42 mmol) and was dissolved in 80 mL of ethanol, and then was added dropwise to the solution of tren and the system refluxed for 36 h under an N_2 atmosphere until the solution lost its red color. Following removal of the solvent by evaporation, water (60 mL) was added to the residue and the solution was extracted with CH_2Cl_2 (60 mL × 3). The combined organic phase was washed twice with water, and then dried over anhydrous Na_2SO_4. The solvent was removed by evaporation, and the residue was purified by column chromatography (silica gel, $CHCl_3$/Methanol/NEt_3 (9/1/1) to afford 1.52 g of a colorless viscous solid, namely intermediate tris(2-aminoethyl)amine-Rhodamine B (**TR**) in a yield of 77.6 %. ^{1}H NMR (500 MHz, $CDCl_3$): δ 7.85 ~ 7.80 (m, 1H, ArH), 7.40 (s, 2H, ArH), 7.05 (s, 1H, ArH), 6.33 ~ 6.24 (m, 6H, ArH), 5.27 (bs, 2H, NCH_2CH_2N), 5.06 ~ 4.08 (bs, 4H, $CH_2CH_2NH_2$), 3.28 (bs, 8H, NCH_2CH_3), 3.11 (bs, 2H, NCH_2CH_2N), 2.92 ~ 2.86 (m, 2H, NCH_2CH_2N), 2.61 ~ 2.55 (m, 2H, NCH_2CH_2N), 2.31 ~ 2.29 (m, 2H, NCH_2CH_2N), 2.10 ~ 2.02 (m, 2H, NCH_2CH_2N), 1.11 (bs, 12H, NCH_2CH_3). ^{13}C NMR (125 MHz, $CDCl_3$): δ 12.2, 37.5, 38.5, 44.0, 51.3, 56.9, 64.8, 97.2, 105.0, 107.7, 122.2, 123.4, 127.8, 128.5, 131.1, 132.0, 148.4, 153.1, 167.4.

The intermediate **TR** (1.10 g, 1.92 mmol) and 2-hydroxy-1-naphthaldehyde (660 mg, 3.84 mmol) were dissolved in methanol (100 mL). The mixture was refluxed overnight under an N_2 atmosphere and then the solvent was removed under reduced pressure, and the residue purified by column chromatography (silica gel, $CHCl_3$) to afford 1.5 g of **TRN** (yellow solid) in yield 85.2 %. Mp: 103.9 ~ 104 °C. ^{1}H NMR (500 MHz, $CDCl_3$) δ (ppm) : 14.14 (s, 2H, OH), 8.59 (s, 2H), 7.93 ~ 7.94 (m, 1H), 7.74 (d, J = 11Hz, 2H), 7.44 ~ 7.53 (m, 6H), 7.31 (t, J = 7.5Hz, 2H), 7.10 ~ 7.15 (m, 3H), 6.76 (d, J = 12.5Hz, 2H), 6.23 ~ 6.43 (m, 6H), 3.42 (t, 4H, J = 6.0Hz), 3.22 ~ 3.28 (m, 10H), 2.69 (t, J = 6.5Hz, 4H), 2.48 (t, J = 8.0Hz, 2H), 1.08 (t, J = 7.5Hz 12H); ^{13}C NMR ($CDCl_3$, 125 MHz):

177.2, 167.6, 158.1, 153.4, 152.9, 148.6, 137.1, 133.7, 132.3, 131.4, 128.9, 128.8, 128.1, 127.7, 125.7, 125.0, 123.8, 122.5, 122.230, 117.808, 107.9, 106.2 105.2, 97.4, 64.9, 54.7 50.8, 50.6, 44.1, 37.5, 30.8 ppm. MS (MALDI-TOF) Calcd for $[C_{56}H_{58}N_6O_4]$: m/z 878.4520 Found: m/z 878.4488 $[M]^+$. (Table S1). The spirolactam form of the Rhodamine B units in **TRN** was confirmed by the presence of a peak at $\delta \sim 64.9$ ppm in the ^{13}C NMR spectrum [43, 44]. (Figs. S1 ~ S3).

3. Results and discussion

3.1 Spectral behavior of probe **TRN**

The skeleton of probe **TRN** is based on the flexible tripod platform and is composed of a Rhodamine B moiety (energy acceptor) and naphthalene moieties (energy donor), which were further covalently connected by a tren linker unit. The emission spectrum of naphthalene and the absorption spectrum of Rhodamine B have substantial overlap, which fulfills a favorable condition for the FRET process (Fig. S4, shaded area).

The emission spectroscopy of probe **TRN** when combined with metal ions was examined in a CH_3CN/H_2O (95/5, v/v) solution of **TRN** (10 μM), in the absence and presence of 20 eq. of various metal ions such as Li^+, Na^+, K^+, Ag^+, Mg^{2+}, Ca^{2+}, Sr^{2+}, Ba^{2+}, La^{3+}, Fe^{3+}, Co^{2+}, Ni^{2+}, Cu^{2+}, Zn^{2+}, Hg^{2+}, pb^{2+}, Cd^{2+}, Al^{3+} and Cr^{3+}. In Fig. 1, the excitation of the initial solution of probe **TRN** at 385 nm showed a slight emission at 445 nm. The addition of Zn^{2+} to the **TRN** solution induced a significant fluorescence emission at 445 nm. On addition of Cu^{2+} to the solution of **TRN**·Zn^{2+}, the fluorescence emission was quenched. However, on addition of Hg^{2+} to a solution of **TRN**, a dramatic fluorescence response was observed. In particular, a new emission peak at 580 nm emerged, no emission band was observed at 445 nm, whilst this was accompanied by an obvious fluorescent color change from colorless to red (Fig. 1 inset). At the same time, on addition of Cu^{2+} to the solution of **TRN**·Hg^{2+}, the fluorescence emission was quenched. It is noteworthy that the addition of Al^{3+} ions resulted in a gradually enhancement of the dual emission at 445 nm and 580 nm on increasing the concentration of Al^{3+}. The emission spectra resulted in an intermediate color between colorless to cherry-red. Therefore, probe **TRN** likely coordinates to the above metal ions. The decrease or increase in the fluorescence of probe **TRN** reveals considerable selectivity for Zn^{2+}/ Al^{3+}/ Hg^{2+} or Cu^{2+}, but no noticeable spectral changes were observed in the presence of the other tested metal ions.

To further understand this mechanism, a detailed investigation was conducted. When Zn^{2+} was added to the solution of probe **TRN** with the

excited wavelength at 385 nm, probe **TRN** exhibited a bright blue fluorescence emission band at 445 nm. The significant fluorescence enhancement was attributed to suppression of C=N isomerization, and the fluorescence increased resulted from chelation-enhanced fluorescence (CHEF). On further addition of Cu^{2+} to the solution of **TRN**·Zn^{2+}, the fluorescence emission was quenched. Addition of Al^{3+} to the solution of probe **TRN** resulted in a gradually enhancement of the dual emission at 445 nm and 580 nm on increasing the concentration of Al^{3+}. The emission spectra resulted in an intermediate color change between colorless to cherry-red. As expected, the spectral results for **TRN**·Al^{3+} exhibited the necessary spectral overlap capable of giving rise to a FRET signal for ring-opened Rhodamine when the naphthalene moiety was excited. The increased emission of the ring-opened Rhodamine at 580 nm was observed with a simultaneously enhanced naphthalene emission at 445 nm. This fluorescence change indicated that a Förster resonance energy transfer (FRET) process from the naphthalene group to the Rhodamine had been triggered by the Al^{3+} ions. However, according to the FRET theory, the naphthalene emission should decrease when such an energy transfer takes place. Given the C=N isomerization process of the complex **TRN**·Al^{3+}, the CHEF may play a more important role than does FRET, thus upon addition of Al^{3+}, enhanced fluorescence of naphthalene is observed. On addition of Cu^{2+} to the solution of **TRN**·Al^{3+}, no change was observed due to the stronger chelation ability of the Al^{3+} ion *versus* the Cu^{2+} ion. Moreover, addition of Hg^{2+} induced only a fluorescence enhancement at 580 nm accompanied by a fluorescent color change of colorless to red (Fig. 1 inset); no emission band was observed at 445 nm. These observations were consistent with an efficient FRET process occurring from the donor (naphthalene) group to the acceptor (Rhodamine) group and suggested the formation of the ring-opened amide form of **TRN** upon binding of the Hg^{2+} ions. On further addition of Cu^{2+} to the solution of **TRN**·Hg^{2+}, the fluorescence emission was quenched. The quenching of Cu^{2+} to **TRN**·Zn^{2+} or **TRN**·Hg^{2+} was not due to the heavy-atom effect because Hg^{2+} did not quench the fluorescence, but is due to the formation of new complexes, which did not emit fluorescence with suitable coordination geometry conformation and cavity size of the receptor [45]. These observations indicate that the probe **TRN** is capable of adopting four different recognition modes. These are dependent on the different target ions present: recognition of Hg^{2+} via the Rh-B moiety (580 nm), Al^{3+} via both the Rh-B (580 nm) and naphthalene moieties (445 nm), whilst Zn^{2+} is only through the naphthalene moiety (445 nm), whilst Cu^{2+} is through both moieties and the formation of a new complex (quenching). Meanwhile, the other metal ions did not

induce any significant fluorescent color change, which suggested that naked-eye selective detection of Zn^{2+}/ Al^{3+}/ Hg^{2+}/ Cu^{2+} under UV-lamp is also possible.

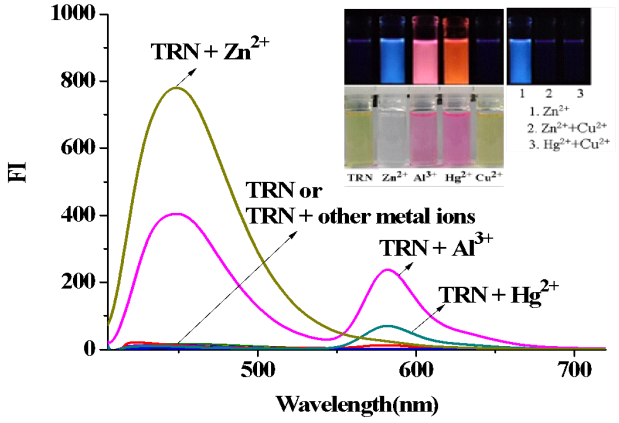

Figure 1. The fluorescence spectrum of probe **TRN** (10 μM) upon the addition of 20 eq. metal ions in CH_3CN/H_2O (95/5, v/v) solution. Metal ions: Li^+, Na^+, K^+, Mg^{2+}, Ca^{2+}, Ba^{2+}, Sr^{2+}, La^{3+}, Hg^{2+}, Pb^{2+}, Cd^{2+}, Al^{3+}, Cu^{2+}, Ni^{2+}, Ag^+, Cr^{3+}, Zn^{2+}, Co^{2+} and Fe^{3+}. λ_{ex}/ λ_{em} = 385/ 445 nm, 580 nm. Inset shows the colour change of probe **TRN** in the absence and the presence of Zn^{2+}/ Al^{3+}/ Hg^{2+} and Cu^{2+} under UV-vis light.

Fig. 2 shows the fluorescence titration of probe TRN with Zn^{2+}, Cu^{2+}, Hg^{2+} and Al^{3+}, respectively. Job's plot experiments evaluated from the fluorescent spectra indicated that the binding of probe **TRN** to Zn^{2+}, Hg^{2+} and **TRN**·Zn^{2+} to Cu^{2+}, are of 1:1 stoichiometry (Fig. 2, inset). The association constants are estimated to be 1.88 × 10^4 M^{-1} (**TRN**·Zn^{2+}), 2.73 × 10^4 M^{-1} (**TRN**·Zn^{2+}·Cu^{2+}), and 1.54 × 10^4 M^{-1} (**TRN**·Hg^{2+}) by using a Benesi-Hildebrand plot assuming a 1:1 stoichiometry, respectively (Fig. S5 ~ S7). The association constants of **TRN**·Al^{3+} are estimated to be 8.60 × 10^8 M^{-2} by using a Benesi-Hildebrand plot assuming a 1:2 stoichiometry (Fig. S8) [46].

From the fluorescence titration, a linear relationship between the emission intensity of **TRN** and ions concentration was observed (Fig. S9 ~ S13).

The detection limit of probe **TRN** for Zn^{2+}, Cu^{2+}, Al^{3+} and Hg^{2+} was calculated based on the fluorescence titration data according to a reported method [47]. Under optimal conditions, calibration graphs for the determination of Zn^{2+}, Cu^{2+}, Al^{3+} and Hg^{2+} were constructed. The limits of detection (LOD = 3σ/ slope) of probe **TRN** for the ions are 0.012 (Zn^{2+}), 0.10 (Hg^{2+}), 0.19 (Al^{3+}: λ_{em} = 445 nm), 0.57 (Al^{3+}: λ_{em} = 580 nm), and **TRN**·Zn^{2+} for Cu^{2+} was 0.01 μM.

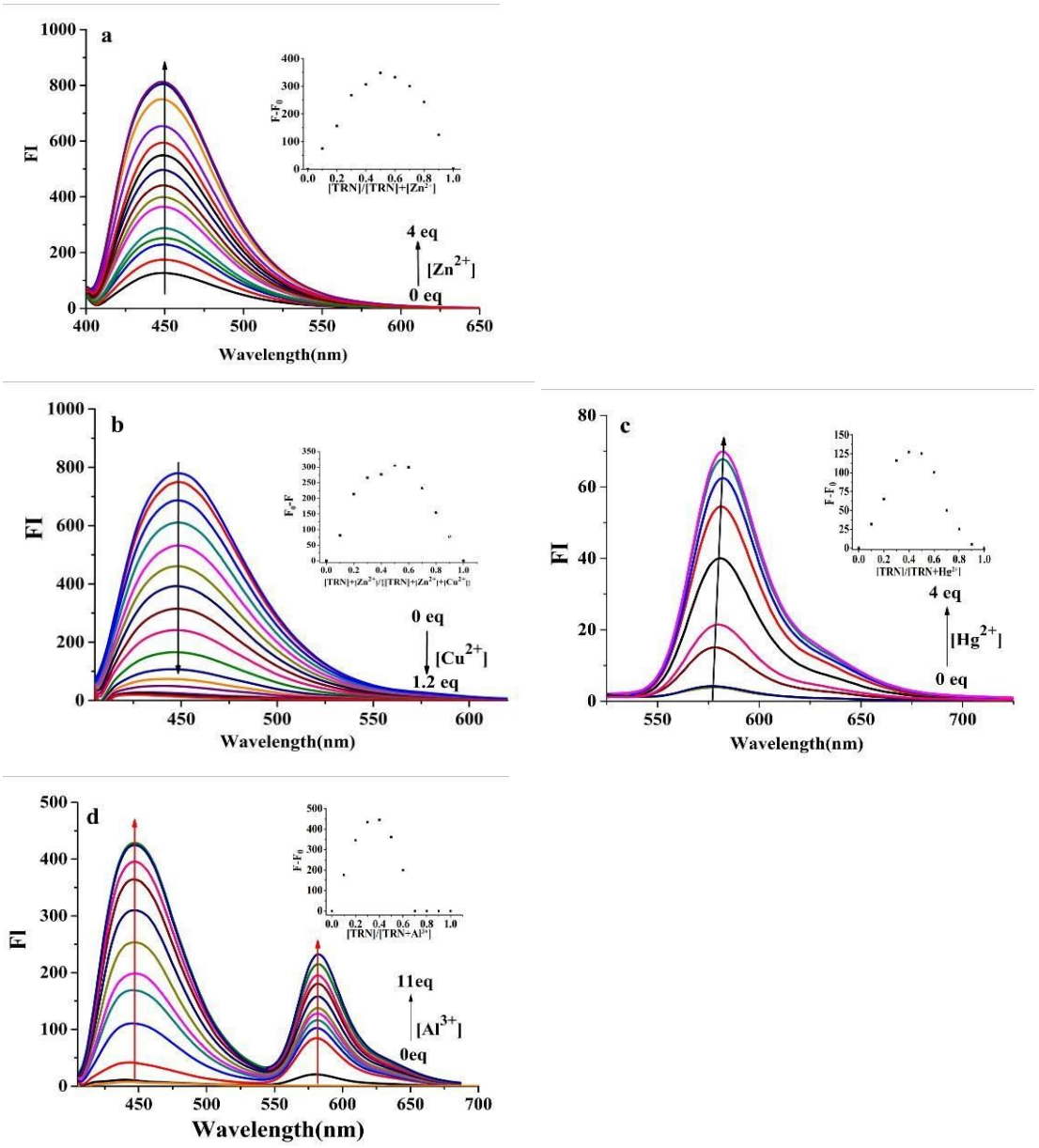

Figure 2. The fluorescence spectral titration of probe **TRN** (10 μM) with Zn^{2+} (a), probe **TRN**·Zn^{2+} with Cu^{2+} (b), probe **TRN** with Hg^{2+} (c) and probe **TRN** with Al^{3+} (d) in CH_3CN/H_2O (95/5, v/v) solution. Inset: the Job's plot data of Zn^{2+} (a, $\lambda_{ex}/\lambda_{em}$ = 385/ 445 nm), Cu^{2+} (b, $\lambda_{ex}/\lambda_{em}$ = 385/ 445 nm), Hg^{2+} (c, $\lambda_{ex}/\lambda_{em}$ = 385/ 580 nm) and Al^{3+} (d, $\lambda_{ex}/\lambda_{em}$ = 385/ 445 nm, 580 nm).

To investigate the practical applicability of **TRN** as a multiple analyte selective fluorescent sensor, competition experiments of **TRN** treated with the detecting ion in the presence of other coexisting ions were conducted. In Fig. S14, it is observed that the other background metal ions had no obvious interference during the detection of Zn^{2+} ions except

for Cu^{2+}, which quenched the fluorescence of **TRN**·Zn^{2+}. In Fig. S15, the other background metal ions had no obvious interference during the detection of Hg^{2+} ions, except for Al^{3+}, which showed a slight interference. In Figs. S16 and S17, the other background metal ions had no obvious interference with the detection of Al^{3+} ions. The **TRN** can distinguished Zn^{2+}/ Al^{3+}/ Hg^{2+} ions through the characteristics of different emission wavelength and double emission. However, no noticeable spectral changes were observed in the presence of the other tested metal ions. Hence, these results suggest that **TRN** could be a good fluorescence enhancement sensor for Zn^{2+}, Hg^{2+} and Al^{3+}, and the probe **TRN** can readily distinguish the above mentioned ions.

3.2 Reaction mechanism of probe **TRN** with Zn^{2+}, Al^{3+} and Hg^{2+}

The binding mode of probe **TRN** with Zn^{2+} was examined by ^1H NMR spectroscopy in CD_3CN. The partial ^1H NMR spectra of probe **TRN** before and after treatment with various concentrations of $Zn(ClO_4)_2$, $Al(ClO_4)_3$ or $Hg(ClO_4)_2$ are depicted in Fig. 3. Complexation of **TRN** with Zn^{2+} shifted the proton of the hydroxyl group (Hb) at δ = 7.92 ppm to 10.87 ppm ($\Delta\delta$ = 2.95 ppm), and the imine proton peak (Ha) at δ = 8.82 ppm was downfield shifted by *ca*. 0.27 ppm. The aromatic protons Hc, Hh, protons of the naphthalene moiety underwent downfield shifts of 0.17 and 0.16 ppm, respectively, due to the reduction of electron density upon coordination to the Zn^{2+} ions. However, the protons associated with the rhodamine moiety exhibited almost no change. These results suggested that the interaction of **TRN** with Zn^{2+} ions is via the nitrogen atoms of the imine and the oxygen atoms of the hydroxyl naphthalene, but that the rhodamine moiety was not involved in the complexation.

Compared with the complexation of tren and Zn^{2+}, upon addition of

Hg^{2+} to the solution of probe TRN, the proton of the hydroxyl group (Hb) on the naphthalene ring shifted downfield from 7.92 ppm to 10.89 ppm ($\Delta\delta$ = 2.97 ppm). The imine proton peak (Ha) at δ = 8.82 ppm was downfield shifted by *ca*. 0.63 ppm, whilst the aromatic protons Hc, and Hh protons of the naphthalene moiety underwent downfield shifts of 0.57 and 0.69 ppm, respectively. Meanwhile, the protons Hm, Hn and Ho on rhodamine moieties exhibited downfield shifts of 0.36, 0.36 and 0.22 ppm, respectively. Aluminum and copper ions revealed the same trend as the mercury ions (See Table S2 for relevant data). These observations strongly suggested that the hydroxyl group, the CH=N moieties of naphthalene and the carbonyl group of rhodamine moieties are all involved in Al^{3+}/ Hg^{2+} coordination. This coordination initiated the FRET process and led to the opening of the spirocycle. The results are consistent with the fluorescence chelation-enhancement and the FRET process occurring. Given this, a mechanism for the sensing of the Zn^{2+}, Al^{3+} and Hg^{2+} ions [48] is proposed in Scheme 2.

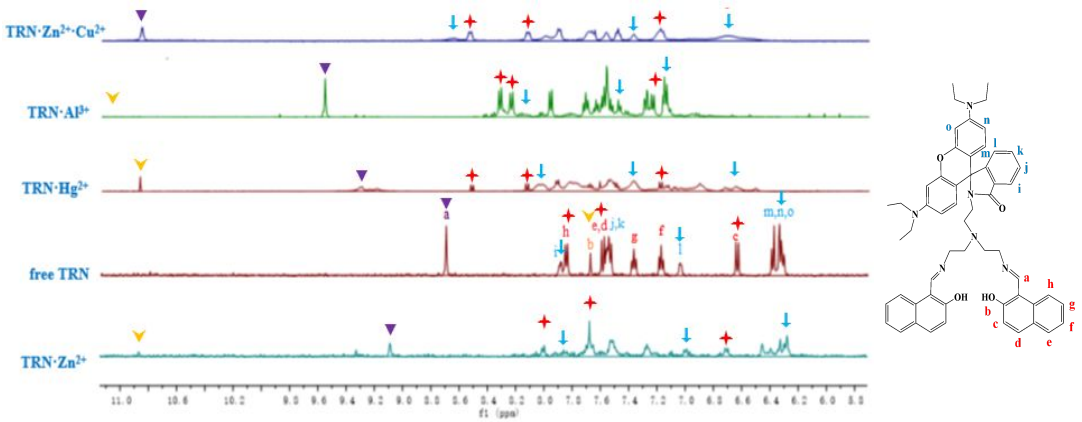

Figure 3. ^{1}H NMR spectra of probe **TRN** in the absence and presence of Zn^{2+}, Hg^{2+}, Al^{3+} and Cu^{2+}. ▽: hydroxy proton, ▼: imine proton, □: aromatic protons of naphthalene moiety, □: protons of rhodamine moieties.

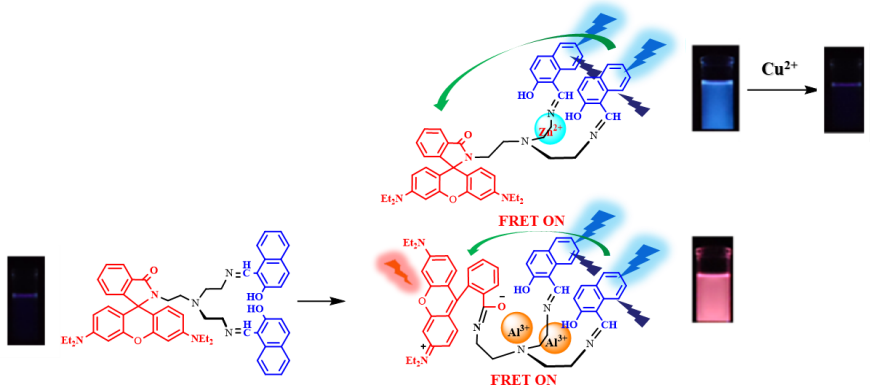

Scheme 2. Proposed sensing mechanism of probe **TRN** with

Zn^{2+}, Hg^{2+}, Al^{3+} and Cu^{2+}.

3.3. PC3 cells imaging applications

The potential application of probe **TRN** for Zn^{2+}, Hg^{2+}, Al^{3+} and Cu^{2+} sensing/imaging in biological samples was investigating through the examination of its interaction with living PC3 cells, using a fluorescent inverted phase contrast microscope. In the control experiment, the PC3 cells were combined with probe **TRN** (10 μM) for 45 min, and resulted in only a negligible intracellular fluorescence (Fig. 3d). Cells incubation with 100 μM of metal ions (Zn^{2+}, Hg^{2+}, Al^{3+} and Cu^{2+}) for 30 ~ 60 min, followed by further treatment with 10 μM probe **TRN** for another 45 min resulted in a significant increase in the fluorescence from the intracellular region (Figs. 3e and f). Bright-field measurements confirmed that the cells, after being treated with Zn^{2+}, Hg^{2+}, Al^{3+} and Cu^{2+} and **TRN**, were viable throughout the dual-channel excited fluorescence imaging experiments. These results demonstrate that the cells are permeable to probe **TRN**, where it binds to intracellular Zn^{2+}, Hg^{2+} and Al^{3+} and emits strong fluorescence. The Cu^{2+} quenches the fluorescence emission of Zn^{2+} and Hg^{2+}, but it does not affect Al^{3+}. Therefore, it is highly suitable for determining the presence of intracellular Zn^{2+}, Hg^{2+}, Al^{3+} and Cu^{2+} ions. The response to Zn^{2+}, Hg^{2+}, Al^{3+} and Cu^{2+} ions, which involves distinctly different colors (blue, red, pink, and colorless, respectively) from the cell samples, raises the prospect that Zn^{2+}, Hg^{2+}, Al^{3+} and Cu^{2+} ions could be simultaneously determined through dual-channel excited fluorescence imaging.

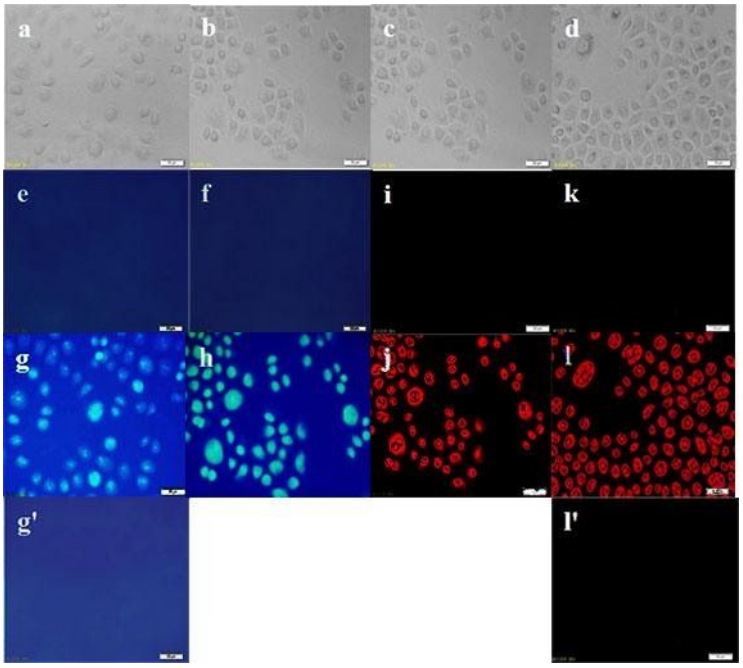

Figure 3. Fluorescence images of PC3 cells on a fluorescent inverted phase contrast microscope. Images were collected at bright field (a ~ d), fluorescent blue channel (λ_{ex} = 330 ~ 385 nm) (e ~ h) and fluorescent red channel (λ_{ex} = 510 ~ 550 nm) (I ~ l). (a, e): The cells were treated with probe **TRN** (10 μM) for 45 min; (g) The cells were first treated with probe **TRN** (10 μM) for 45 min and further treated with Zn^{2+} (100 μM) for another 60 min; (g') The cells of g were further treated with Cu^{2+} (100 μM) for another 60 min; (b, c, f, i): The cells were treated with probe **TRN** (10 μM) for 45 min; (h, j) The cells were first treated with probe **TRN** (10 μM) for 45 min and further treated with Al^{3+} (100 μM) for another 60 min; (d, k): The cells were incubated with probe **TRN** (10 μM) for 45 min; (l) The cells were first treated with probe **TRN** (10 μM) for 45 min and further treated with Hg^{2+} (100 μM) for another 30 min. (l') the cells of probe **TRN** were further treated with Cu^{2+} (500 μM) for another 50 min.

4. Conclusion

The results herein suggest that probe **TRN** is an excellent single molecular sensor, which can detect Zn^{2+}, Hg^{2+}, Al^{3+} and Cu^{2+} with dissimilar emission bands and by the naked-eye. The fluorescence data also indicate that probe **TRN** can be used in living systems for the detection of Zn^{2+}, Hg^{2+}, Al^{3+} and Cu^{2+} levels. This new strategy for sensing multi-analytes is based on the flexible tripod platform. Therefore, probe **TRN** is expected to become a useful chemical sensor in the field of environmental monitoring or medical investigations. Our study illustrates an effective and novel strategy to differentiate multi-analytes. This work provides a promising new strategy for the simultaneous detection of ions by one simple probe.

Acknowledgements

We are grateful for the financial support from the Natural Science Foundation of China (No. 51663005). CR thanks the EPSRC for financial support (Overseas Travel award EP/R023816/1).

References

[1] M. Shahid, S. Khalid, I. Bibi, J. Bundschuh, N.K. Niazi, C. Dumat, A critical review of mercury speciation, bioavailability, toxicity and detoxification in soil-plant environment: ecotoxicology and health risk assessment, Sci. Total Environ. 711 (2019) 134749.

[2] W. Sun, S.-G. Guo, C. Hu, J.-L. Fan, X.-J. Peng, Recent development of chemosensors based on cyanine platforms, Chem. Rev. 116 (2016) 7768-7817.

[3] S. Kumari, Amit, R. Jamwal, N. Mishra, D. K. Singh, Recent Developments in Environmental Mercury Bioremediation and its Toxicity: A Review, Environmental Nanotechnology, Monitoring & Management. 13（2020）100283.

[4] D. Altschuh, S. Oncul, A.P. Demchenko, Fluorescence sensing of intermolecular interactions and development of direct molecular biosensors, J. Mol. Recognit. 19 (2006) 459-477.

[5] E. Ho, DNA damage, cancer risk, J. Nutr. Biochem. 15 (2004) 572-578.

[6] S.C. Burdette, S.J. Lippard, Meeting of the minds: metalloneurochemistry, Proc. Natl. Acad. Sci. USA. 100 (2003) 3605-3610.

[7] J. Wu, W. Liu, J. Ge, H. Zhang, P. Wang, New sensing mechanisms for design of fluorescent chemosensors emerging in recent years, Chem. Soc. Rev. 40 (2011) 3483-3495.

[8] C. J. Frederickson, J.Y. Koh, A.I. Bush, The neurobiology of zinc in health and disease, Nat. Rev. Neurosci. 6 (2005) 449-462.

[9] J. L. Smith, S. Xiong, W. R. Markesbery, M. A. Lovell, Altered expression of zinc transporters-4 and-6 in mild cognitive impairment, early and late Alzheimer's disease brain, Neuroscience. 140 (2006) 879-888.

[10] E. Ho, Zinc deficiency, DNA damage and cancer risk, Nutr. Biochem. 15 (2004) 572-578.

[11] R. A. Sladek, A genome-wide association study identifies novel risk loci for type 2 diabetes, Nature. 445 (2007) 881-885.

[12] P. Verwilst, K. Sunwoo, J. S. Kim, The role of copper ions in pathophysiology and fluorescent sensors for the detection thereof, Chem. Commun. 51 (2015) 5556-5571.

[13] P. Nayak, impacts and disease, Environ. Res. 89 (2002) 101-115;

[14] G. Berthon, Metal ions in neurological systems, Coord. Chem. Rev. 228 (2002) 319-341.

[15] T. V. O'Halloran, V. C. Culotta, Metallochaperones, an intracellular shuttle service for metal ions, J. Biol. Chemy. 275 (2000) 25057-25060.

[16] A. C. Rosenzweig, T. V. O'Halloran, Structure and chemistry of the copper chaperone proteins, Curr. Opin. Chem. Biol. 4 (2000) 140-147.

[17] S. Puig, D. J. Thiele, Molecular mechanisms of copper uptake and distribution, Curr. Opin, Chem. Biol. 6 (2002) 171-180.

[18] Z.-Y. Xu, Q.-Y. Meng, Q. Cao, Y.-S. Xiao, H. Liu, G. Han, S.-H. Wei, J. Yan, L.-D. Wu, Selective Sensing of Copper Ions by Mesoporous Porphyrinic Metal-Organic Frameworks Nanoovals, Anal. Chem. 92 (2020) 2201-2206.

[19] Q. Gao, L. Ji, Q.-N. Wang, K. Yin, J.-H. Li, L.-Xin. Chen, Colorimetric sensor for highly sensitive and selective detection of copper ion, Anal. Method. 9 (2017) 5094-5100.

[20] H. Yu, W. Zhao, Y. Zhou, G.-J. Cheng, M. Sun, L. Wang, L. Yu, C. Ran, S.-H. Liang, Salen-based bifunctional chemosensor for copper (II) ions: Inhibition of copper-induced amyloid-β aggregation, Analytica Chimica Acta. 1097 (2020) 144-152.

[21] S. Li, D. Zhang, X. Xie, S. Ma, Y. Liu, Z. Xu, Y. Ye, A novel solvent-dependently bifunctional NIR absorptive and fluorescent ratiometric probe for detecting Fe^{3+}/Cu^{2+} and its application in bioimaging, Sens. Actuators, B. 224 (2016) 661-667.

[22] M.-J. Yuan, W.-D. Zhou, X.-F. Liu, M. H.-Y. Zhu, Z.-C. Yin, Z.-C. Zheng, H.-B. Yang, Y.-L. Liu, Y.-L. Li, D.-B. Zhu, A multianalyte chemosensor on a single molecule: promising structure for an integrated logic gate, J. Org. Chem. 73 (2008) 5008-5014.

[23] H.-H. Song, Z. Zhang, A quinoline-based ratiometric fluorescent probe for discriminative detection of Zn^{2+} and Cd^{2+} with different binding modes, and its Zn^{2+} complex for relay sensing of pyrophosphate and adenosine triphosphate, Dyes Pigm. 165 (2019) 172-181.

[24] W. Wang, Q. Wen, Y. Zhang, X.-L. Fei, Y.-X. Li, Q.-B. Yang, X.-Y. Xu, Simple naphthalimide-based fluorescent sensor for highly sensitive and selective detection of Cd^{2+} and Cu^{2+} in aqueous solution and living cells, Dalton. Trans. 42 (2013) 1827-1833.

[25] J. Hana, X. Tang, Y. Wang, R. Liu, L. Wang, L. Ni, A quinoline-based fluorescence "on-off-on" probe for relay identification of Cu^{2+} and Cd^{2+} ions, Spectrochim. Acta. Part A. 205 (2018) 597-602.
[26] Q. Zhua, L. Liua, Y.-P. Xing, X.-H. Zhou, Duplex functional G-quadruplex/NMM fluorescent probe for label-free detection of lead (II) and mercury (II) ions, J. Hazard. Mater. 355 (2018) 50-55.
[27] S. Gharami, K. Aich, L, Patraa, T. K. Mondal, Detection and discrimination of Zn^{2+} and Hg^{2+} using a single molecular fluorescent probe, New J. Chem. 42 (2018) 8646-8652.
[28] T. Anand; B. Vinita, S. K. Suban, A multi-analyte selective dansyl derivative for the fluorescence detection of Cu (ii) and cysteine, Photochem. Photobiol. 18 (2019) 1533-1539.
[29] M. Banerjee, M. Ghosh, S. Ta, J. Das, D. Das, A smart optical probe for detection and discrimination of Zn^{2+}, Cd^{2+} and Hg^{2+} at nano-molar level in real samples, J. Photochem. Photobiol A. 377 (2019) 286-297.
[30] F. Ye, N. Wu, P. Li, Y.-L. Liu, S.-J. Li, A lysosome-targetable fluorescent probe for imaging trivalent cations Fe^{3+}, Al^{3+} and Cr^{3+} in living cells, Spectrochim. Acta. Part A. 222 (2019) 1386-1425.
[31] R. Alam, R. Bhowmick, A. S. M. Islam, A. katarkar, K. Chaudhuri, M. Ali, A rhodamine based fluorescent trivalent sensor (Fe^{3+}, Al^{3+}, Cr^{3+}) with potential applications for live cell imaging and combinational logic circuits and memory devices, New J. Chem. 41 (2017) 8359-8369.
[32] T. Rasheed, C.-L. Li, Y.-L. Zhang, F. Nabeel, J.-X. Peng, J. Qi, L.-D. Gong, C.-Y. Yu, Rhodamine-based multianalyte colorimetric probe with potentialities as on-site assay kit and in biological systems, Sens. Actuators, B. 258 (2018) 115-124.
[33] N. Kumar, V. Bhalla, M. Kumar, Resonance energy transfer-based fluorescent probes for Hg^{2+}, Cu^{2+} and Fe^{2+}/Fe^{3+} ions, Analyst. 139 (2014) 543-558.
[34] J. Tang, S. Ma, D. Zhang, Y. Liu, Y. Zhao, Y. Ye, Highly sensitive and fast responsive ratiometric fluorescent probe for Cu^{2+} based on a naphthalimide-rhodamine dyad and its application in living cell imaging, Sens. Actuators, B. 236 (2016) 109-115.
[35] K. E. Sapsford, L. Berti, I. L Medintz, Materialien für den resonanten Fluoreszenzenergietransfer (FRET): jenseits klassischer Donor-Acceptor-Kombinationen, Angew. Chem. 118 (2006) 4676-4704.
[36] L. Yuan, W. Lin, K. Zheng, FRET-based small-molecule fluorescent probes: rational design and bioimaging applications, Accounts. Chem. Res, 46 (2013) 1462-1473.
[37] C. Kaewtong, J. Noiseephum, Y. Uppa, A reversible Em-FRET rhodamine-based chemosensor for carboxylate anions using a ditopic receptor strategy, New. J. Chem. 34 (2010) 1104-1108.
[38] X. Chen, T. Pradhan, F. Wang, J. S. Kim, J. Yoon, Fluorescent chemosensors based on spiroring-opening of xanthenes and related derivatives, Chem. Rev. 112 (2012) 1910-1956
[39] M. Li, Y. Li, X. Wang, X. Cui, T. Wang, Synthesis and application of near-infrared substituted rhodamines, Chinese. Chem. Lett. 30 (2019) 1682-1688.
[40] X. Chen, T. Pradhan, F. Wang, Fluorescent chemosensors based on spiroring-opening of xanthenes and related derivatives. Chem. Rev, 112 (2012) 1910-1956.
[41] M. J. Chang, K. Kim, K. S. Park, J. S. Kang, C. S. Lim, H. M. Kim, C. Kang, M. H. Lee, High-depth fluorescence imaging using a two-photon FRET system for mitochondrial pH in live cells and tissues, Chem. Commun. 54 (2018) 13531-13534.
[42] S. R. Gupta, P. Yadav, P. Singh, B. Koch, V. P. Singh, A "Turn-On" Fluorescence Probe for Selective Detection of Al^{3+} in Aqueous Environment: Crystal Structure, Theoretical and Cell Imaging Studies, ChemistrySelect. 5 (2020) 2284 -2290.
[43] S. Erdemir, S. Malkondu, O. Kocyigit, A reversible calix[4]arene armed phenolphthalein based fluorescent probe for the detection of Zn^{2+} and an application in living cells, Luminescence. 34 (2019) 106-112.
[44] Z. Li, J.-L. Zhao, Y.-T. Wu, L. Mu, X. Zeng, Z. Jin, G. Wei, N. Xie, C. Redshaw, Highly selective recognition of Al^{3+} and I^- ions using a bi-functional fluorescent probe, Org. Biomol. Chem. 15 (2017) 8627-8633.

[45] B. Biswal, A. Pal, B. Bag, Two-step FRET mediated metal ion induced signalling responses in a probe appended with three fluorophores, Dalton Trans. 46 (2017) 8975-8991.
[46] Y. Wang, P. -D. Mao, W.-Na. Wu, X.-Jie. Mao, Y.-C. Fan, X.-L. Zhao, Z.-Q. Xu, Z.-H. Xu, New pyrrole-based single-molecule multianalyte sensor for Cu^{2+}, Zn^{2+}, and Hg^{2+} and its AIE activity, Sens. Actuators, B. 255 (2018) 3085-3092.
[47] Q. Ruan, L. Mu, X. Zeng, J.-L. Zhao, L. Zeng, C. Redshaw, A three-dimensional (time, wavelength and intensity) functioning fluorescent probe for the selective recognition/discrimination of Cu^{2+}, Hg^{2+}, Fe^{3+} and F^{-} ions, Dalton Trans. 47 (2018) 3674-3678.
[48] M. H. Lee, H. J. Kim, S. Yoon. N. Park. J. S. Kim, Metal ion induced FRET OFF-ON in Tren/Dansyl-appended rhodamine, Org. Lett. 10 (2008) 213-216.